Journal of Applied Fluid Mechanics, Vol. 13, No. 1, pp. 299-315, 2020.
Available online at www.jafmonline.net, ISSN 1735-3572, EISSN 1735-3645.
DOI: 10.29252/jafm.13.01.29891

Modelling VOCs Emissions in Coal Fired Power Stations using Perfectly Stirred Reactor Approach

Ö. Arslan

Mechanical Engineering Department, Muş Alparslan University, MSU Kampusu, Muş 49250, Turkey

†*Corresponding Author Email: o.arslan@alparslan.edu.tr*

(Received December 5, 2018; accepted May 18, 2019)

ABSTRACT

The main objective of this study is to evaluate the emissions of volatile organic compounds (VOCs) from coal-fired power stations. A quantitative understanding of the chemistry controlling the formation and destruction of these intermediate species is a prerequisite for the realistic modelling of pollutant formation in flames. Therefore, well investigated skeletal reaction mechanism has been built and introduced into perfectly stirred reactor model in order to accomplish prediction of some of these hazardous important intermediate species. This can be great help in considering lack of experimental VOCs data from fossil fuel fired power stations. Predicted results have been validated against ICSTM Furnace data where possible. The performance of the model against the large laboratory scale experimental data has resulted in considerable confidence in the use of this model for a full-scale boiler configuration. But, more confidence will be forthcoming from an increase in the amount of validation data, which is unluckily lacking at the moment. Furthermore, the model can be used in order to provide deeper insight into the formation processes of VOC species emitted from coal-fired power stations. However, this can be accomplished far better by including more elementary reactions into the skeletal reaction mechanism.

Keywords: VOCs; PAHs; Power stations; PSR model; Toxic; Carcinogens.

NOMENCLATURE

i	number of the species
k_f	the forward rate constant of elementary reaction n
k_b	the backward rate constant of elementary reaction n
w_i	concentration of i species
W_i	molecular weights of i species
$\dot{w}_i$	chemical production or consumption rate for species i
Y_{vol}	volatile source
Y_i	mass fraction of species i at time t
Yi^*	mean value of the i species in that particular cell
$Z_{c,vol}$	mass fraction of carbon in the volatiles
ω_n	the molar reaction rate of a specific elementary reaction $\nu'_{i,n}$ &$\nu''_{i,n}$ the stoichiometric coefficients
τ	the nominal residence time
dYi/dt	the net consumption or production of species i in the calculating domain

1. INTRODUCTION

Coal combustion is the most widespread manner of fossil energy utilisation for power production. Coal is either blended with other waste fuels, burned alone or co-fired with biomass etc. In spite of its fundamental importance, its greatest drawback is the pollutants that are generated during combustion and the post combustion disposal of the solid residue. These important pollutants may be classified into four groups; NOx, SOx, unburned hydrocarbons (VOCs and PAHs) and solids (ash, particulate matter). In general, any attempt to reduce the formation of certain emissions may encourage the formation of the others. Extensive experimental and modelling work has been undertaken on NOx and SOx such as Hassan (1997), Wei *et al.* (2012) and Kang *et al.* (2015). However, relatively less research has been conducted on VOCs, since an understanding of

incomplete hydrocarbon combustion is a far more complex subject. The same time the development of an understanding of the mechanisms of formation and reduction of NOx and SOx was a first priority.

There are extensive possible VOCs species existent in coal combustion. Therefore, it is important to identify the most abundant and hazardous VOCs in coal fired power stations. To this end, an extensive literature survey has been conducted in order to identify these species for tackling this issue more effectively. However, the main problem faced in this area is a very limited available data (Masclet *et al*., 1987; Garcia *et al*., 1992; Fernandez-Martinez *et al.*, 2001). These data are generally restricted to total volatile and non volatile PAHs or total hydrocarbons (Revuelta *et al.*, 1999; Pisupati *et al.*, 2000). Some species were investigated individually in only a few studies of large scale power plant such as Garcia *et al*. (1992) and in small scale pilot plant Chagger *et al.* (1999). This fact is probably related to the difficulties in sampling and accurately determining volatile organics in real emissions (Arslan, 2015, Harrison, 2002).

The other important issue is that majority of VOCs species are intermediate species. To understand the underlying principles of how these pollutants are formed, we should thoroughly understand the reaction mechanisms involved in combustion processes. In this work a skeletal reaction mechanism has been developed in order to predict VOCs emission for pulverised coal combustion. The skeletal reaction mechanism consists of 97 elementary reactions and 41 species and comprises C_1-C_6 compounds. For modelling, the concept of a perfectly stirred reactor (PSR) is appended as a 'post-processor' to the FAFNIR in house built CFD code. FAFNIR. This model is shortly called as PSR-VOC. In this model each finite cell volume is assumed to be a perfectly stirred reactor and the constructed skeletal reaction mechanism is applied for evaluation of VOCs emissions. This model can be used as a tool to predict the most abundant and hazardous VOC species from coal burned power stations such as benzene, formaldehyde and 1,3-butadiene etc.

2. BACKGROUND IN HOUSE BUILT CFD CODE, FAFNIR

The discretisation and solution of the general transport equations are well-established. Detailed information on various methods can be found in Patankar (1980), Versteeg and Malalasekera (2007), Ferziger and Peric (2013) and other standard fluid dynamics textbooks. These books give all the necessary means to be able to construct a successful model and solve it.

The model (PSR-VOC) developed here is embedded as a post-processor of a well-established CFD code, FAFNIR, which is an ICSTM in-house developed CFD code. An account of the various stages of its development can be found in Lockwood *et al*. (1980), Rizvi (1985), Levy (1991) and Yehia (1992). The FAFNIR code is structured around numerical methods that can tackle thermo-fluid flow problems. It is a combination of three elements; namely the pre-processor FEEDER, a main program and a post-processor for graphics output. The pre-processor FEEDER was developed by Levy (1991) and Yehia (1992). It reads and interprets all of the information required by the main program in the SEED in a standard format.

The main program is constructed by applying well established following methods over the time. The kinetics of fluid flow, gas species and heat transfer are modelled applying an Eulerian method. Later they derived into general transport equations. A standard k-ε model (Launder and Spalding, 1974) is used for the modelling of turbulence. The hybrid scheme is used to discretise the differential forms of the momentum transport equation. A Lagrangian method is employed for the evaluations of mean particle trajectories in the flow domain by supposing finite starting locations of a finite number of particle size groups. The momentum, heat and mass transfer between the particle and gas phases are evaluated applying the particle source in cell (PSIC) method. A single reaction model (Anthony and Howard, 1976) is employed for the particle devolatilisation. An eddy dissipation model (Magnussen and Hjertager, 1976) is used to determine the rate of volatile combustion. The Non-Equilibrium Diffusion Radiation Model (Gibb, 1973) is used to estimate the radiation effects on energy transport on gas, particles and wall boundaries.

FAFNIR has been validated against pulverised coal data from a number of furnaces of different sizes, such as the ICSTM furnace (Lockwood and Mahmud, 1988; Costa *et al*., 1990; Lockwood and Romo-Millares, 1992 etc), the furnaces at the IFRF, the CCRL test facilities (Lockwood and Salooja, 1983; Abbas and Lockwood, 1988) and an industrial cement kiln (Lockwood and Shen, 1994).

3. ASSEMBLING THE VOC-SKELETAL REACTION MECHANISM

The skeletal reaction mechanism has been constructed directly from relevant literature for the purpose of accurate prediction of important VOCs emanating from the pulverised coal combustion (diffusion flame) and choosing the related elementary reaction steps according to those species. In the VOCs-skeletal reaction mechanism not only degradation but also formation of higher hydrocarbon species from the small precursors recombination are well thought-out. The following part is briefly devoted to approach taken towards the construction of the VOC-skeletal reaction mechanism. The proposed reaction mechanism is justified from relevant literature as well.

Important species and reactions are chosen from relevant works, which are representative for initiation, chain branching, and termination steps for C_1-C_6 species in methane and acetylene combustion. This is done in order to accurately predict concentrations of some important

intermediate and hazardous volatile hydrocarbon species, such as 1, 3-butadiene, benzene and formaldehyde emissions. Some of the reactions in the VOCs-skeletal reaction mechanism represent the basic reaction mechanism for C_1-C_2 hydrocarbon combustion and important radicals such as H, O and OH. The remaining reactions describe the formation and destruction of higher hydrocarbons containing up to six carbon atoms. All reactions are assumed to be reversible with the reverse rates calculated from the appropriate equilibrium constants. Because of the combustion system of interest, namely the ICSTM Furnace, atmospheric conditions apply. This is represented by k_0 index. Furthermore in this skeletal reaction mechanism, high temperature products are chosen for some elementary reactions in order to evaluate emission of high temperature turbulence combustion environment species correctly. Nonetheless the same reactants may have different products in a low temperature environment.

For the construction of the VOC-skeleton mechanism Warnatz's (1981, 1992) reaction paths namely, rich methane-air flame, lean methane-air flame and stoichiometric benzene-air flame reaction paths are mainly used. These reactions paths give a solid foundation for establishing important species and the direction reactions proceeding from possible reaction branches. Rich methane-air flame and lean methane-air flame give an insight into C_1-C_2 combustion, while stoichiometric benzene air flame reaction path is for C_6-C_4 (benzene) combustion. Furthermore, C_4 and C_3 combustion species and elementary reactions mainly were derived from the works of Lueng (1995), Lueng and Lindstedt (1995) and Lindstedt and Skevis (1994, 1997). They point out differences between pre-mixed and non-premixed flames and show the importance of recombination in some elementary reactions for forming higher hydrocarbon species in the nature of diffusion flames. Moreover, some of the important reactions are taken from benzene oxidation of Tregrossi *et al.* (1999), Righter *et al.* (1999) and Righter and Howard (2000). For the radical generation and chain branching, most of the reaction steps are taken from Seshdari and Peters (1988, 1990), Lueng and Linsted (1995), Smooke (1991), Warnatz (1981, 1992) and Rogg (1988). Alkemade and Homann (1989) and Lueng and Lindstedt (1995) suggested that benzene is formed by the propargyl radical self-recombination. This process is probably a major source of "the first aromatic ring" in the combustion of hydrocarbons. The significance of the C_3 recombination path is also supported by the high concentrations of propargyl radical observed in fuel-rich flames. According to Lueng (1995)'s the kinetic simulation, the reduction in benzene concentration is mainly as a result of phenyl radical decomposition, rather than its oxidation or molecular growth.

The formation of benzene increases in the main oxidation zone of the flame and reaches its maximum just before the flame front. The higher temperature in front of the flame and the increase in radical species favour benzene decomposition, which causes a decrease in its net formation rate. In the present mechanism, all these various paths are considered to assess their relative importance in different conditions. According to Richter *et al.* (1999) and Lueng (1995), the modelling of the growth of higher PAHs requires reasonably good predictions for smaller intermediates since some of these intermediates act as precursors. The same time, accurate predictions of key radical species, such as H, O and OH, are also essential. Therefore, the C_1-C_2 reaction mechanism plays an important role. Furthermore, the mechanisms which lead to the production of PAHs and other VOCs in the combustion process are complex because models involving stepwise reactions of small species and aromatics species. These species may combine to form higher molecular weight PAHs (Chagger *et al.*, 1999; Wang and Frenklach, 1997). Moreover, Tregrossi *et al.* (1999) have shown the most abundant species in the benzene flame, which are in the following order; C_2H_2, CH_4, C_4H_4, C_3H_4, and C_4H_6 (1,3-butadiene). In addition, they claim that the other species occur in very small amounts, such as C_3H_4 (1,2 propadine), C_3H_6 (propane), C_2H_6 (ethane) and C_4H_6 (1-buteyne), in the combustion chamber.

The construction strategy for the VOC skeletal reaction mechanism is to first choose the most important and abundant species from relevant works. The second step is to determine how these species can be generated with the aid of a sub-mechanism. Thirdly, the most important species and formation and destruction paths for these sub-mechanism fuels are determined. Finally, some very important elementary reaction steps are chosen in order to produce vital reaction initiating radicals, such as H, OH, O etc. This is very crucial for initiating the next elementary reaction, while the overall reaction mechanism should produce an accurate concentration of the radicals for the success of the multi-step reaction mechanism. The VOC-skeletal reaction mechanism consists of 41 species and 97 reactions. A complete referenced list of the reaction mechanism and related kinetic information can be found in Table 1.

4. MODELLING OF VOCS SPECIES USING PERFECTLY STIRRED REACTOR

The well-stirred reactor was first used as a combustion research tool by Longwell and Weiss (1955). Before that PSR were limited to lower temperature (<1200 K) applications. At these lower temperatures stirred reactors create an excellent basis for a comparative study of the relative rates of decomposition, addition and abstraction reactions. However, later on stirred reactors were applied at temperatures exceeding 1600 K (i.e. as Lam *et al.*, 1991; Marr *et al.*, 1994; Vaughn *et al.*, 1991; Takahashi *et al.*, 1995) which is a realistic value for typical turbulent diffusion flames. Apart from the basic chemical kinetics calculations, the idea of a well-stirred reactor has also been applied in turbulent combustion (Yamazaki and Ichigava,

Table 1 VOCs Skeletal Mechanism (97 Elementary Reactions)

No	Reactions			A (m^3, Kmol, s^{-1})	n	E (KJ/mol)	Ref.
1	$H + O_2$	⇔	$OH + O$	2.000E+11	0.00	70.34	Baulch *et al.* (1992)
2	$O + H_2$	⇔	$OH + H$	5.120E+01	2.67	26.30	Baulch *et al.* (1992)
3	$OH + H_2$	⇔	$H_2O + H$	1.000E+05	1.60	13.80	Baulch *et al.* (1992)
4	$2OH$	⇔	$H_2O + O$	1.500E+06	1.14	0.42	Baulch *et al.* (1992)
5	$O_2 + H + M$	⇔	$HO_2 + M^a$	2.300E+12	-0.80	0.00	Warnatz (1984)
6	$HO_2 + H$	⇔	$2OH$	1.686E+11	0.00	3.66	Baulch *et al.* (1992)
7	$HO_2 + OH$	⇔	$H_2O + O_2$	2.890E+10	0.00	-2.08	Baulch *et al.* (1992)
8	$HO_2 + O$	⇔	$OH + O_2$	3.190E+10	0.00	0.00	Baulch *et al.* (1992)
9	$CO + OH$	⇔	$CO_2 + H$	6.320E+03	1.50	-2.08	Baulch *et al.* (1992)
10	$CO + HO_2$	⇔	$CO_2 + OH$	1.500E+11	0.00	98.93	Tsang&Hampson (1986)
11	$CH + O_2$	⇔	$CHO + O$	3.300E+10	0.00	0.00	Baulch *et al.* (1992)
12	$CH + CO_2$	⇔	$CHO + CO$	3.400E+09	0.00	2.90	Baulch *et al.* (1992)
13	$CH + H_2O$	⇔	$CH_2O + H$	1.170E+12	-0.75	0.00	Miller&Melius (1992)
14	$CH + C_2H_2$	⇔	$c\text{-}C_3H_2 + H$	1.785E+11	0.00	-0.51	Skevis (1996)
15	$CHO + M$	⇔	$CO + H + M^b$	1.860E+14	-1.00	71.10	Timonen *et al.* (1987)
16	$CHO + H$	⇔	$CO + H_2$	9.000E+10	0.00	0.00	Baulch *et al.* (1992)
17	$CHO + O$	⇔	$CO + OH$	3.000E+10	0.00	0.00	Baulch *et al.* (1992)
18	$^1CH_2 + M$	⇔	$^3CH_2 + M^d$	1.000E+08	0.00	0.00	Lueng (1995)
19	$^1CH_2 + H_2$	⇔	$CH_3 + H$	7.230E+10	0.00	0.00	Tsang&Hampson (1986)
20	$^1CH_2 + C_2H_2$	⇔	$C_3H_3 + H$	1.800E+11	0.00	0.00	Miller&Melius (1992)
21	$^3CH_2 + H_2$	⇔	$CH_3 + H$	3.000E+06	0.00	0.00	Baulch *et al.* (1992)
22	$^3CH_2 + H$	⇔	$CH + H_2$	1.100E+11	0.00	0.00	Böhland&Temps (1984)
23	$^3CH_2 + OH$	⇔	$CH + H_2O$	1.130E+04	2.00	12.56	Miller&Melius (1992)
24	$^3CH_2 + C_2H_2$	⇔	$C_3H_3 + H$	1.200E+10	0.00	27.70	Miller&Melius (1992)
25	$CH_2O + H$	⇔	$CHO + H_2$	2.288E+07	1.05	13.70	Baulch *et al.* (1992)
26	$CH_2O + O$	⇔	$CHO + OH$	4.150E+08	0.57	11.56	Baulch *et al.* (1992)
27	$CH_2O + OH$	⇔	$CHO + H_2O$	3.400E+06	1.18	-1.87	Baulch *et al.* (1992)
28	$CH_3 + O$	⇔	$CH_2O + H$	8.430E+10	0.00	0.00	Baulch *et al.* (1992)
29	$CH_3 + OH$	⇔	$CH_3O + H$	1.500E+11	0.00	34.46	Grotheer *et al.* (1992)
30	$CH_3 + OH$	⇔	$^1CH_2 + H_2O$	4.000E+10	0.00	20.47	Grotheer *et al.* (1992)
31	$2CH_3$	⇔	$C_2H_5 + H$	1.800E+09	0.10	4.44	Lueng (1995)
32	$2CH_3$	⇔	C_2H_6, k_0	1.270E+35	-7.00	11.55	Baulch *et al.* (1994)
33	$CH_3O + M$	⇔	$CH_2O + H + M$	5.450E+10	0.00	56.50	Grotheer *et al.* (1992)
34	$CH_3O + H$	⇔	$CH_2O + H_2$	2.000E+10	0.00	0.00	Tsang&Hampson (1986)
35	CH_4	⇔	$CH_3 + H$, k_0	8.430E+14	0.00	379.95	Baulch *et al.* (1992)
36	$CH_4 + H$	⇔	$CH_3 + H_2$	1.325E+01	3.00	33.63	Baulch *et al.* (1992)

37	$CH_4 + OH$	⇔	$CH_3 + H_2O$	1.560E+02	1.83	11.60	Lueng (1995)
38	$C_2H + H_2$	⇔	$C_2H_2 + H$	4.074E+02	2.40	0.84	Kiefer *et al.* (1992)
39	$C_2H + O_2$	⇔	$2CO + H$	3.520E+10	0.00	0.00	Miller&Melius (1992)
40	$C_2H + OH$	⇔	$CHCO + H$	2.000E+10	0.00	0.00	Miller&Melius (1992)
41	$C_2H + O$	⇔	$CO + CH$	1.000E+10	0.00	0.00	Baulch *et al.* (1992)
42	$CHCO + O_2$	⇔	$2CO + OH$	4.000E+09	0.00	3.57	Baulch *et al.* (1992)
43	$CHCO + H$	⇔	$^1CH_2 + CO$	1.500E+11	0.00	0.00	Baulch *et al.* (1992)
44	$CHCO + O$	⇔	$^2CO + H$	1.000E+10	0.00	0.00	Lueng (1995)
45	$C_2H_2 + O$	⇔	$^3CH_2 + CO$	2.170E+02	2.10	6.57	Lueng (1995)
46	$C_2H_2 + O$	⇔	$CHCO + H$	5.060E+02	2.10	6.57	Lueng (1995)
47	$C_2H_2 + OH$	⇔	$C_2H + H_2O$	6.000E+10	0.00	54.00	Lueng (1995)
48	$C_2H_2 + OH$	⇔	$C_2H_2O + H$	1.100E+08	0.00	30.00	Lueng (1995)
49	$C_2H_2O + H$	⇔	$CHCO + H_2$	5.000E+10	0.00	33.50	Miller&Melius (1992)
50	$C_2H_2O + H$	⇔	$CH_3 + CO$	1.130E+10	0.00	14.40	Miller&Melius (1992)
51	$C_2H_2O + OH$	⇔	$CHCO + H_2O$	7.500E+09	0.00	8.37	Miller&Melius (1992)
52	C_2H_3	⇔	$C_2H_2 + H$, k_o	4.155E+38	-7.50	190.39	Baulch *et al.* (1994)
53	$C_2H_3 + O_2$	⇔	$C_2H_2 + HO_2$	4.000E+08	0.00	0.00	Westmoreland (1992)
54	$C_2H_3 + C_2H_2$	⇔	(1,3)-C_4H_5	9.300E+35	-8.76	50.24	Wang&Frenklach (1994)
55	$2C_2H_3$	⇔	(1,3)-C_4H_6	2.000E+10	0.00	0.00	Benson (1989)
56	$C_2H_4 + H$	⇔	$C_2H_3 + H_2$	5.420E+11	0.00	62.35	Baulch *et al.* (1992)
57	$C_2H_4 + OH$	⇔	$C_2H_3 + H_2O$	2.047E+10	0.00	24.86	Baulch *et al.* (1992)
58	$C_2H_5 + M$	⇔	$C_2H_4 + H + M$	2.000E+12	0.00	125.60	Westbrook&Pitz (1984)
59	$C_2H_5 + O$	⇔	$CH_3 + CH_2O$	6.600E+10	0.00	0.00	Baulch *et al.* (1992)
60	$C_2H_6 + H$	⇔	$C_2H_5 + H_2$	1.445E+06	1.50	31.00	Baulch *et al.* (1992)
61	$C_2H_6 + O$	⇔	$C_2H_5 + OH$	1.000E+06	1.50	24.30	Baulch *et al.* (1992)
62	$C_2H_6 + OH$	⇔	$C_2H_5 + H_2O$	7.226E+03	2.00	3.61	Baulch *et al.* (1992)
63	$c\text{-}C_3H_2 + OH$	⇔	$C_2H_2 + CO + H$	5.000E+10	0.00	0.00	Miller&Melius (1992)
64	$c\text{-}C_3H_2 + O_2$	⇔	$C_2H_2 + CO_2$	2.000E+07	0.00	0.00	Lueng (1995)
65	C_3H_2O	⇔	$C_2H_2 + CO$	8.510E+14	0.00	297.00	Michael and Lim (1993)
66	$C_3H_3 + H$	⇔	$c\text{-}C_3H_2 + H_2$	5.000E+10	0.00	0.00	Lueng&Lindstedt (1995)
67	$C_3H_3 + O$	⇔	$C_3H_2O + H$	1.400E+11	0.00	0.00	Slagle *et al.* (1990)
68	$C_3H_3 + OH$	⇔	$C_3H_2O + H_2$	1.000E+10	0.00	0.00	Lueng (1995)
69	$C_3H_3 + {}^3CH_2$	⇔	$C_4H_4 + H$	4.000E+10	0.00	0.00	Miller&Melius (1992)

70	$C_3H_3+C_3H_3$	⇔	C_6H_5+H	3.000E+09	0.00	0.00	Violi *et al.* (1999)
71	$C_3H_3+C_3H_3$	⇔	C_6H_6	1.000E+08	0.00	0.00	Wang&Frenklach (1997)
72	C_4H_2 + O	⇔	CO + c-C_3H_2	2.800E+10	0.00	7.23	Homann&Wellmann(1983)
73	n-C_4H_3	⇔	i-C_4H_3	1.500E+13	0.00	163.30	Lueng (1995)
74	n-$C_4H_3+C_2H_2$	⇔	C_6H_5	9.600E+67	-17.77	131.00	Wang&Frenklach (1994)
75	i-C_4H_3	⇔	C_4H_2+H, k_0	2.000E+12	0.00	200.83	Miller&Melius (1992)
76	i-C_4H_3 + H	⇔	C_4H_2 + H_2	5.000E+10	0.00	0.00	Miller&Melius (1992)
77	i-C_4H_3 + OH	⇔	C_4H_2 + H_2O	3.000E+10	0.00	0.00	Miller&Melius (1992)
78	C_4H_4 + H	⇔	n-C_4H_3 + H_2	2.000E+04	2.00	25.17	Lueng (1995)
79	C_4H_4 + OH	⇔	n-C_4H_3 + H_2O	1.000E+04	2.00	12.60	Lueng (1995)
80	(1,3)$C_4H_5+C_2H_2$	⇔	C_6H_6 + H	1.600E+13	-1.33	22.60	Wang&Frenklach (1994)
81	(1,3)-C_4H_6	⇔	i-C_4H_5+ H	4.200E+15	0.00	414.21	Lueng (1995)
82	i-C_4H_5	⇔	C_4H_4+H, k_0	2.000E+15	0.00	175.73	Miller&Melius (1992)
83	(1,3)-C_4H_6+H	⇔	(1,3)-C_4H_5 + H_2	6.300E+07	0.70	25.10	Weissman&Benson (1988)
84	(1,3)-C_4H_6+H	⇔	C_2H_3+ C_2H_4	5.000E+08	0.00	0.00	Kiefer *et al.* (1985)
85	(1,3)-C_4H_6+OH	⇔	(1,3)-C_4H_5 + H_2O	8.380E+09	0.00	-3.89	Liu *et al.* (1988)
86	C_5H_5 + O	⇔	(1,3)-C_4H_5 + CO	1.000E+11	0.00	0.00	Emdee *et al.* (1992)
87	C_5H_5 + O	⇔	C_5H_5O	1.000E+10	0.00	0.00	Bittker(1991)
88	C_5H_5O	⇔	(1,3)-C_4H_5 + CO	2.510E+11	0.00	183.68	Emdee *et al.* (1992)
89	C_6H_5 + O_2	⇔	C_6H_5O + O	2.090E+09	0.00	31.25	Bittker(1991)
90	C_6H_5O	⇔	C_5H_5 + CO	4.500E+11	0.00	183.68	Lin & Lin(1986)
91	C_6H_6	⇔	C_6H_5 + H	4.570E+13	0.00	372.37	Kern *et al.* (1985)
92	C_6H_6 + H	⇔	C_6H_5 + H_2	2.500E+11	0.00	66.99	Kiefer *et al.* (1985)
93	C_6H_6 + O	⇔	C_6H_5 + OH	2.000E+10	0.00	61.52	Leidreiter&Wagner (1989)
94	C_6H_6 + O	⇔	C_6H_5OH	2.400E+10	0.00	19.53	Leidreiter&Wagner (1989)
95	C_6H_6 + OH	⇔	C_6H_5 + H_2O	1.630E+05	1.42	6.10	Baulch *et al.* (1992)
96	C_6H_5OH +H	⇔	C_6H_5O + H_2	1.150E+11	0.00	51.92	Emdee *et al.* (1992)
97	C_6H_5OH+ OH	⇔	C_6H_5O + H_2O	6.000E+09	0.00	0.00	Emdee *et al.* (1992)

Here Reaction Mechanism Rate Coefficients in the Form $k_j = AT^n\exp(-E/RT)$
All third-body collision efficiencies are equal to unity unless otherwise stated.

[a] M : Enhanced Collision Efficiencies : H_2O = 6.5; O_2 =0.3; CO = 0.7; CO_2 = 1.5; N_2 = 0.4

[b] M : Enhanced Collision Efficiencies : H_2O = 12.0; H_2 =2.5; CO = 1.9; CO_2 = 3.8

[c] M : Collision Efficiencies for H_2O , H_2 and CO_2 are excluded

[d] M : Enhanced Collision Efficiencies : H_2O = 4.0; N_2 =0.4; CO = 0.4; CO_2 = 0.4; CH_4 = 0.7; C_2H_2 = 1.4; C_2H_6 = 2.2

1970; Villermaux, 1986; Fox and Villermaux, 1990; Mantel and Borghi, 1994). Borghi (1988) explains in detail where the perfectly stirred reactor approach can be implemented in turbulent combustion systems. This justification is not a necessary criterion for the present work since the PSR is implemented as a post-processor and the main program, FAFNIR, manages the turbulent combustion calculation.

For modelling purposes, the concept of a perfectly stirred reactor (PSR) is appended as a 'post-processor' to the CFD code. In this model each finite cell volume is assumed to be a perfectly stirred reactor. The PSR model requires the important assumption that the rate of conversion from reactants to products is controlled by the chemical reaction rates and not by the mixing processes. Since mixing processes are assumed to be infinitely fast, the mathematical description is written ignoring all the details inside the reactor. As a consequence, no spatial temperature and concentration gradients are involved in each finite volume, which is assumed to represent a perfectly stirred reactor. The dependent variables, such as concentration and temperature, are not functions of position and hence all fluid properties within the reactor are identical at all locations and at all times. These assumptions greatly simplify the calculations in systems of interest, such as turbulent combustion systems or chemical industry applications.

4.1 Construction of the PSR-VOC Model

Apart from the fast mixing, the modelling of a well-stirred reactor requires additional assumptions. Firstly, the flow through the reactor must be characterised by a nominal residence time, which can be deduced from the flow rate and reactor volume. In the present work the nominal residence time is represented by the turbulent kinetic energy over the eddy viscosity (k/ε). This defines the residence time in turbulent combustion flow as being the time a species stays in a specific finite volume.

The PSR-VOC model treats each finite element as an independent well-stirred reactor. Every stirred reactor has a different temperature, volume etc., which are evaluated by the FAFNIR. The layout of this model begins with the assumptions on the initial fuel value in a finite volume, descriptions of the set of algebraic equations describing the well-stirred reactor and calculations of species concentrations for each time step. This is followed by the description of the numerical method, DVODE, which solves the ordinary 'stiff' and 'non-stiff' ordinary differential equation.

It is very important to have some qualitative expectation of the combustion environment, when a suitable reaction mechanism is constructed according to the nature of the problem, such as coal combustion. The present assumption based on experimental data from the large-scale ICSTM Furnace (Abbas, 1993), in which the fuel is initially released as methane and acetylene mixture. Abbas's results show that the most abundant species are similar to intermediate products of methane and acetylene fuel mixture combustion products, such as CH_3, C_3H_3 etc. Laboratory scale chemical kinetics research on combustion provides further interval steps through the reaction path. These interval steps produce intermediate species that are mostly pollutants. According to these species, the relevant important elementary reactions are selected in the previous section in order to establish the VOCs-skeletal reaction mechanism for this work.

This VOC-skeletal reaction mechanism has been constructed for the accurate prediction of important VOC's species concentration in pulverised coal flames. This mechanism comprises species up to C_6 and is used in the PSR model. PSR model is subsequently integrated with the FAFNIR main program as a post processor. In the post processor, 'PSR-VOC', the prediction of the most hazardous and abundant VOCs can be made. The following is an explanation of the PSR-VOC model, which has been developed in this work.

Initial mass concentrations of methane and acetylene are evaluated based on two main assumptions:

1) The first approach is based on the experimental data of Abbas (1993), which indicates that most of the unburned hydrocarbon species in the gas phase are similar to those of the intermediate species of a methane and acetylene flame.

2) Furthermore, it is assumed that the rate of formation of the initial species in the combustor, e.g., methane and acetylene, are proportional to the concentration of volatile matter as follows:

$$w_{C_2H_2} = 0.7 \times Y_{vol} Z_{C,vol} \left(\frac{W_{C_2H_2}}{W_C}\right) \quad (1)$$

$$w_{CH_4} = 0.3 \times Y_{vol} Z_{C,vol} \left(\frac{W_{CH_4}}{W_C}\right) \quad (2)$$

here, w_{C2H2} and w_{CH4} are the concentration of acetylene, and methane (kg/m^{3}s), respectively, Y_{vol} is the volatile source(kg/ m^{3}s), W_{C2H2}, W_{CH4} and W_C are molecular weights of acetylene, methane and carbon, respectively. $Z_{c,vol}$ is the mass fraction of carbon in the volatiles, 0.7 and 0.3 represent the ratios of the initial values of acetylene and methane concentrations in each finite volume, respectively.

The reaction rate ω_n for the elementary reaction n can be written as:

$$\omega_n = k_{f,n}(T)\prod_{i=1}^{N}\left(\frac{Y_i\rho}{W_i}\right)^{v'_{i,n}} - k_{b,n}(T)\prod_{i=1}^{N}\left(\frac{Y_i\rho}{W_i}\right)^{v''_{i,n}} \quad (3)$$

Here the mass fraction of the species involved is converted to molar concentration since the value of the initial species is evaluated as a mass fraction in the main code:

Here $v'_{i,n}$ and $v''_{i,n}$ denote the stoichiometric coefficients, i denotes the number of the species,

w_i represents the molecular weight of species *i*, k_f and k_b, denote the forward and backward rate constant of elementary reaction *n*. Y_i denotes mass fraction and ω_n is the molar reaction rate of a specific elementary reaction.

The net chemical reaction rate for species *i* contains contributions from all elementary reactions ($n,...K$) involving *i* species and can be expressed as:

$$\dot{w}_i = \sum_{n=1}^{K} (\nu''_{i,n} - \nu'_{i,n})\omega_n \quad (4)$$

Subsequently, we can use the perfectly stirred reactor equations to calculate the amount of every species in the reaction zone.

$$\frac{d(Y_{mole})_i}{dt} = -\frac{(Y)_i - (Y)_i^*}{\tau} + \frac{\dot{w}_i}{\rho_{mix}} w_i \quad (5)$$

where *Yi* denotes mass fraction of species *i* at time t and *Yi** is mean value of the *i* species in that particular cell. $\dot{w}_i$ denotes chemical production or consumption rate for species *i* and contains contributions from all related elementary reactions, in which the calculating species is involved. w_i denotes the molecular weight of *i* species (*kg/kmol*). τ is the nominal residence time which corresponds to (k/ε) in turbulence combustion. Finally, *dYi/dt* represents the net consumption or production of species *i* in the calculating domain.

4.2 Calculation Balance Equation for Species

To deduce the formation and consumption reactions for each species in the VOC-skeletal mechanism, the system of balance equations for each species is formulated from Eq. (4), i.e.

$$\begin{aligned}\dot{w}_O = {} & \omega_1 - \omega_2 + \omega_4 - \omega_8 + \omega_{11} - \omega_{17} - \omega_{26} \\ & - \omega_{28} - \omega_{41} - \omega_{44} - \omega_{45} - \omega_{46} - \omega_{59} \\ & - \omega_{61} - \omega_{67} - \omega_{72} - \omega_{86} - \omega_{87} + \omega_{89} \\ & - \omega_{93} - \omega_{94}\end{aligned}$$

Here each number represents the relevant elementary reaction from the reaction mechanism scheme. The net reaction rate of the individual elementary reaction rate, which corresponds with the number, is evaluated by Eq. (3).

4.3 Numerical Solution of Ordinary Differential Equations

Species mass fractions change according to a set of simultaneous ordinary differential equations (ODE's). These equations, although possibly stiff due to their rather large coefficients, could be readily treated via the various solutions methods, such as Runge-Kutta and Euler's Method. However, in the solution of simultaneous systems of equations more sophisticated methods need to be used, such as the explicit methods of Adams-Bashforth and the implicit methods of Adams-Moulton. More information can be found on most of the applicable numerical methods in the standard textbooks, such as Diprima and Boyce (2012) and Burden *et al.* (2015). Fortunately, there is no need to write a program since there is a well-established and efficient program, the DVODE (Brown *et al.*, 1989) that can be implemented in the present work.

DVODE stands for Variable-coefficient Ordinary Differential Equation solver, with fixed-leading coefficient implementation, with D denoting double precision. DVODE solves the initial value problem for 'stiff' or 'non-stiff' systems of first order ODEs. The DVODE was developed and improved for better efficiency and stability over two decades. All this development work can be found in the literature such as (such as, Byrne and Hindmarsh, 1975, 1976; Hindmarsh and Byrne, 1977; Hindmarsh, 1983). DVODE is a well known ODE solver can be found in (http://netlib.sandia.gov/ode/vode.f).

The initial action of the DVODE code is to determine (or guess) whether or not the problem is 'stiff. Stiffness occurs when the Jacobian matrix, df/dy, has an eigenvalue whose real part is negative and large in magnitude, compared to the reciprocal of the t span of interest. According 'stiffness' status, a suitable flag (MF) needs to be assigned, briefly shown below.

Values of the MF method flag are:

10 for non-stiff (Adams) method, no Jacobian used.

21 for stiff (BDF) method, externally supplied full Jacobian.

22 for stiff method, internally generated full Jacobian.

24 for stiff method, externally supplied banded Jacobian.

25 for stiff method, internally generated banded Jacobian.

If the problem is 'non-stiff', a method flag MF = 10 is applied. If it is stiff, there are four standard choices for MF (21, 22, 24, 25), and DVODE requires the Jacobian matrix in some form. The Jacobian matrix is regarded either as full (MF = 21 or 22), or banded (MF = 24 or 25). In the banded case, DVODE requires two half-bandwidth parameters, ML and MU. Supplying the Jacobian directly (MF = 21 or 24) is advised. But if this is not feasible, DVODE will compute it internally by difference quotients by assigning MF = 22 or 25.

5. Results And Discussion

In this section pulverised coal combustion predictions are represented in two subsequent sections. In the first section, the experimental data of two different coal combustion measured in the furnace are compared with predictions obtained from the FAFNIR. And then the PSR-VOC model predictions are presented and compared data where possible. The contents of two coals, namely Kellingly and Gedling, are given with operating conditions of experimental set up (Tables 2-4). Both

varieties are UK-sourced. The Gelding coal combustion experiment was conducted by Abbas (1993). The Kellingly coal combustion experiment was done by Harrison (2002). These experimental results were collected from the ICSTM furnace, using the SAO burner configuration. Description of the ICSTM furnace and the experimental methods for the measurement of pulverised coal combustion and co-combustion can be found in the works of Abbas (1993), Costa (1992), Hassan (1997) and Harrison (2002) etc.

Table 2 Characteristics of Gedling & Kellingly coals (Abbas, 1993; Harrison, 2002)

	Coal type	
	Gedling	Kellingly
Proximate analysis:	(% mass)	(% mass)
Volatiles	35.8	31.4
Fixed carbon	53.7	51.9
Moisture	6.3	3.5
Ash	4.2	13.2
Ultimate analysis:	(% mass)	(% mass)
Carbon	72.6	69.04
Hydrogen	5.05	4.41
Nitrogen	1.29	1.51
Sulphur	1.55	1.83
Oxygen	15.31	5.92
Chlorine	---	0.58
Particle size distribution:	(% mass)	(% mass) est.
0-10 µm.	15.0	16.4
10-25 µm.	25.0	20.0
25-45 µm.	20.0	20.0
45-75 µm.	20.0	20.0
>75 µm.	20.0	18.6
Gross calorific value, MJ/kg	29.29	29.113

Table 3 Furnace Operating Conditions (Abbas, 1993; Harrison, 2002)

	Coal	
Central Pipe:	Gedling	Kellingly
Air flow rate, kg/s	2.777×10^{-4}	2.700×10^{-4}
Swirl number	0.0	0.0
Temperature, K	353	298
Coal feed rate, kg/s	0.39×10^{-2}	0.3934×10^{-2}
Primary:		
Air flow rate, kg/s	8.833×10^{-3}	9.500×10^{-3}
Swirl number	0.0	0.0
Temperature, K	353	298
Secondary:		
Air flow rate, kg/s	3.344×10^{-2}	3.280×10^{-2}
Swirl number	1.03	1.03
Temperature, K	573	600
Excess air (%)	15	15

Table 4 Kinetic Parameters for Coal Combustion Modelling (Abbas, 1993; Harrison, 2002).

Kinetic parameters:	E (j/kg-mol)	k_0, K_0
Devolatilisation	7.4×10^{7}	8.36×10^{4} s^{-1}
Char reaction	1.02×10^{8}	0.86 kg.s.N/m^4

5.1 Combustions Results and their Validations

The predicted aerodynamic flow pattern and particle trajectories for the Gedling and Kellingly coal are shown in Figs. 1-4 respectively. The common observation of all these graphs is the reverse zone flow induced by the swirl in the near burner region (NBR). The IRZ holds back coal particles and reverses their trajectories towards the burning zone. With the aid of this process, intense and efficient mixing occurs between the forward flow of the secondary stream and the reverse flow. This process makes it possible for the coal particles to devolatilise in this high temperature region. The trajectories of the particles undergoing the devolatilisation process in the combustion chamber are shown by the dotted lines in Figs. 3 and 4. This devolatilisation process supplies gas species in this area where combustion and chemical reaction occur in the gas phase. This produce a high energy release. Hence this provides the necessary high temperature for an efficient and self-stabilising mechanism for ignition throughout the combustion phenomena. The predictions of the main CFD code, FAFNIR, show that most of the remaining char is ignited in the oxygen-rich region of the secondary jet since the process keeps the largest particles within IRZ. Thereby this increases residence time for heterogeneous combustion, with the necessary oxygen being supplied by the secondary air stream.

It should be noted that the flow pattern obtained for the Gedling coal case in Fig. 1 is very similar to that obtained for the Kellingly coal, shown in Fig. 2. This implies that the volatile content of the coal has little or no effect on the aerodynamic features of the corresponding flame. Figures 5 and 6 show temperature-contours while Figs. 7 and 8 depict the oxygen profiles for Gedling and Kellingly coal combustion, respectively. The quality of the predictions are reasonably accurate, especially in the near burner zone where most of the combustion takes place. Figures 9 and 11 for Gedling coal and Figs. 10 and 12 for Kellingly coal (only one axial station) show comparisons between the predictive and experimental profiles of gas temperature and oxygen concentration.

It can be seen that there is a drastic decrease in oxygen concentration close to the burner axis at stations of x/d=1.1 and 2.2. Here x is the displacement from the quarl exit and d is the diameter of secondary air stream. This is due to intensive volatile combustion in the recirculation zone near the burner, as can be seen from the oxygen contour (Fig.s 7 and 8). The prediction of low and uniform values of oxygen concentration in the external recirculation zone approximately 1.5 diameters from the axis of the furnace suggests that oxygen consumption is insignificantly small. And the transportation of the mixture downstream is due to the convection and diffusion processes.

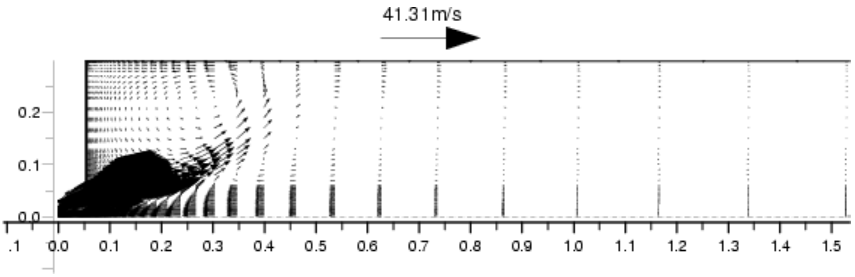

Fig. 1. Predicted Velocity Vectors for Gedling coal.

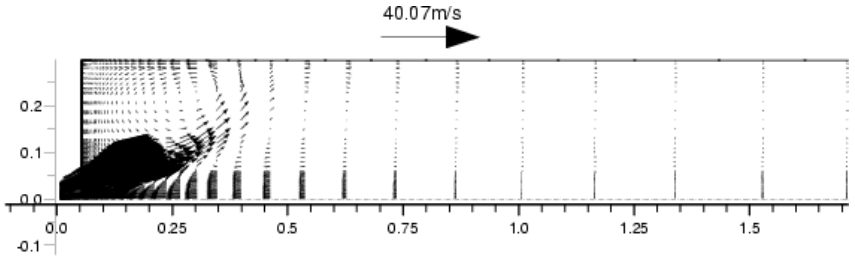

Fig. 2. Predicted Velocity Vectors for Kellingly coal.

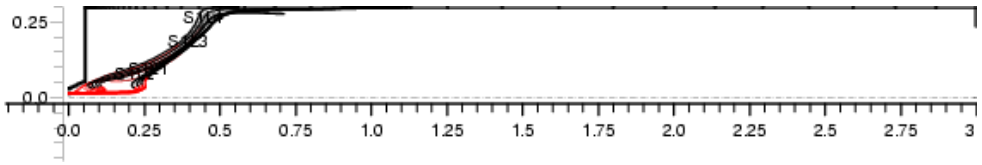

Fig. 3. Predicted Particle Trajectories in the NBR for Gedling coal.

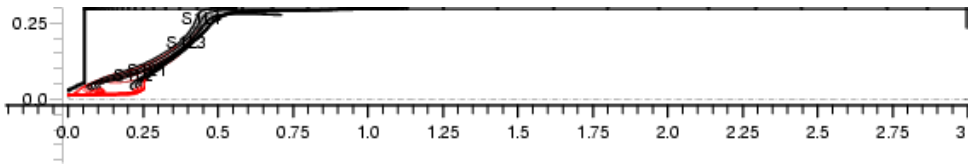

Fig. 4. Predicted Particle Trajectories in the NBR for Kellingly coal.

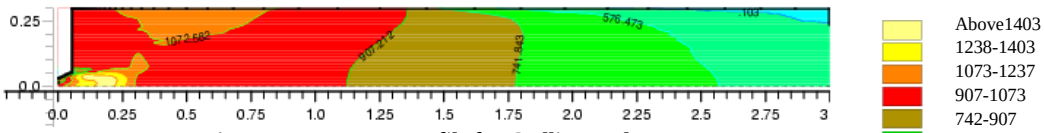

Fig. 5. Temperature Profile for Gedling coal.

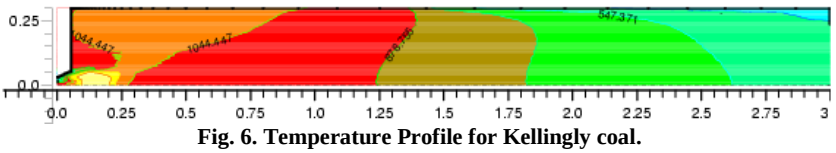

Fig. 6. Temperature Profile for Kellingly coal.

The slight over-prediction of the concentration in the external recirculation zone and up to an x/d = 12.9 downstream can be seen. This appears to indicate an under-prediction of the consumption rate of oxygen close to the final stages of char combustion. Despite the differences between prediction and measurement, the crucial locations of the combustion zone, the recirculation and the secondary jet flow in the near burner zone are well-predicted. The differences at stations further downstream of the burner are small. However, this can be neglected with some degree of confidence.

The peak temperature in the region corresponding to the internal recirculation zone is the result of the high energy storage in the torroidal vortex situated between the secondary jet and the internal

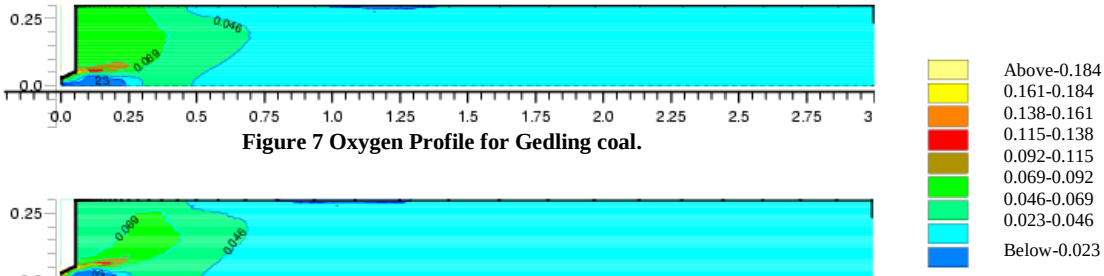

Figure 7 Oxygen Profile for Gedling coal.

Figure 8 Oxygen Profile for Kellingly coal.

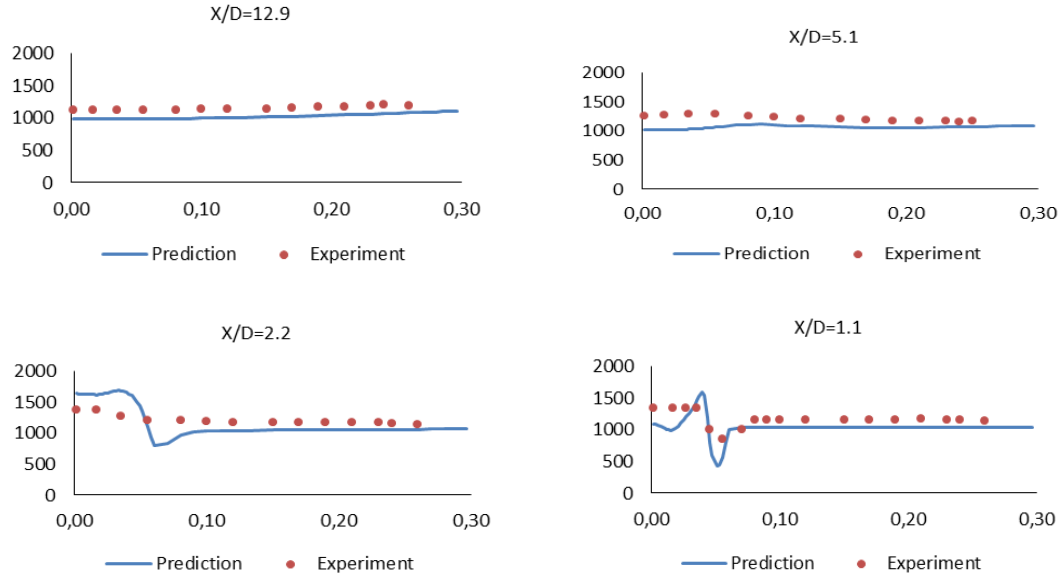

Fig. 9. Validation of the Radial Temperature (C^0) Profiles for Gedling coal.

recirculation zone. A steep decrease, followed by a relatively flat profile (at x/d = 1.1 and 2.2) indicate the locations of the secondary jet and the external recirculation, respectively. The measurement of high and evenly distributed temperatures of the combustion products in the external recirculation zone suggest the effectiveness of the thermal insulation of the wall.

However, it is important to note the over-predicted temperatures around the centre of the internal recirculation zone (at x/d = 2.2). This can be the result of a more intense distribution of predicted temperatures in the IRZ which takes place in a region more confined than those suggested by the measurements. A slight under-prediction of temperature occurs at x/d = 1.1 and 2.2. This is an indication of an underestimation of the heat diffusion effects on the transport of energy. This is probably due to deficiencies in the turbulence heat transfer. However, these discrepancies do not have a major affect on the predictive quality of the model in general.

Finally, if we compare the accuracy of the temperature and oxygen with each other, the predicted gas temperatures are generally in better agreement with the data. The discrepancy observed in the oxygen concentrations at x/D = 2.2 is also reflected in the predicted gas temperatures.

5.2 VOCs Results and their Validations

Prior to discussing the predictions of VOCs, it is instructive to delineate the combustion environment created by the aforementioned SAO type burner. Especially in the near burner region (NBR) of SAO is important since most of the volatiles are released here. Hence these volatile matters cause formation or destruction reactions influencing pollutant emissions. In Figs. 1 and 2, the velocity vectors in the NBR, where a strong internal recirculation zone (IRZ) is near the furnace axis. Secondary air forward flow is at the burner quarl exit and relatively weak external recirculation zone is the prominent feature typically associated with the swirl-stabilised coal flames. The medium size particles (50+µm) spend approximately10-20 ms in the relatively oxygen-lean environment prior to being entrained into the oxygen-rich high shear zone between the IRZ boundary and the secondary air stream.

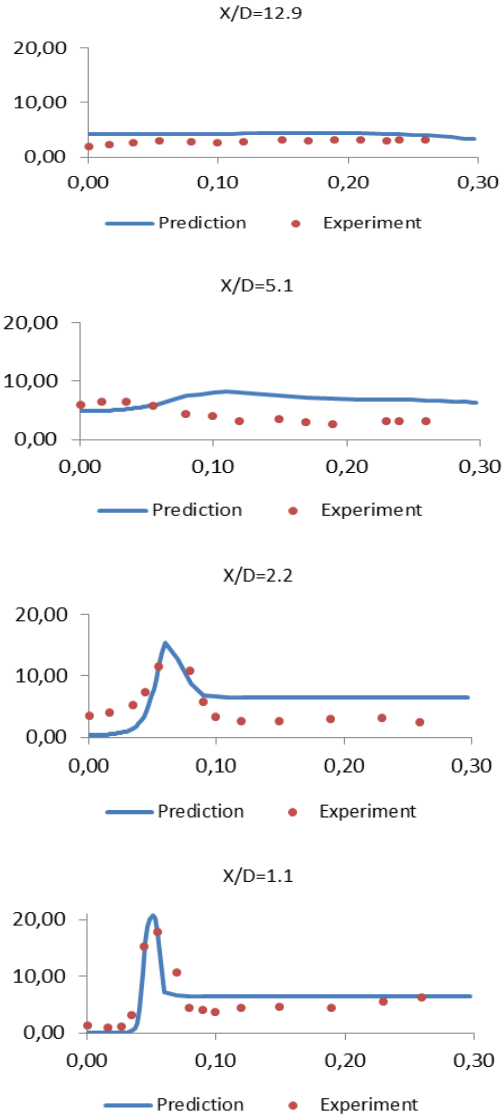

Fig. 10. Validation of Oxygen Concentration (%) for Gedling coal.

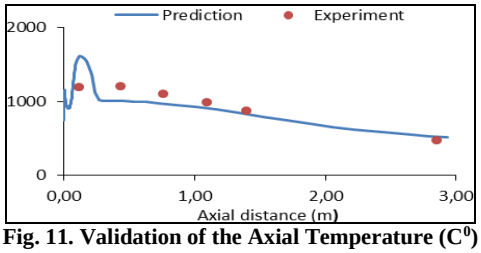

Fig. 11. Validation of the Axial Temperature (C^0) Profile for Kellingly coal.

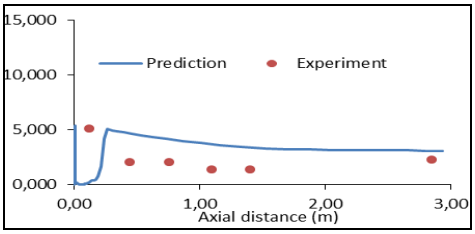

Fig. 12. Validation of the Axial Oxygen Concentration (%) for Kellingly coal.

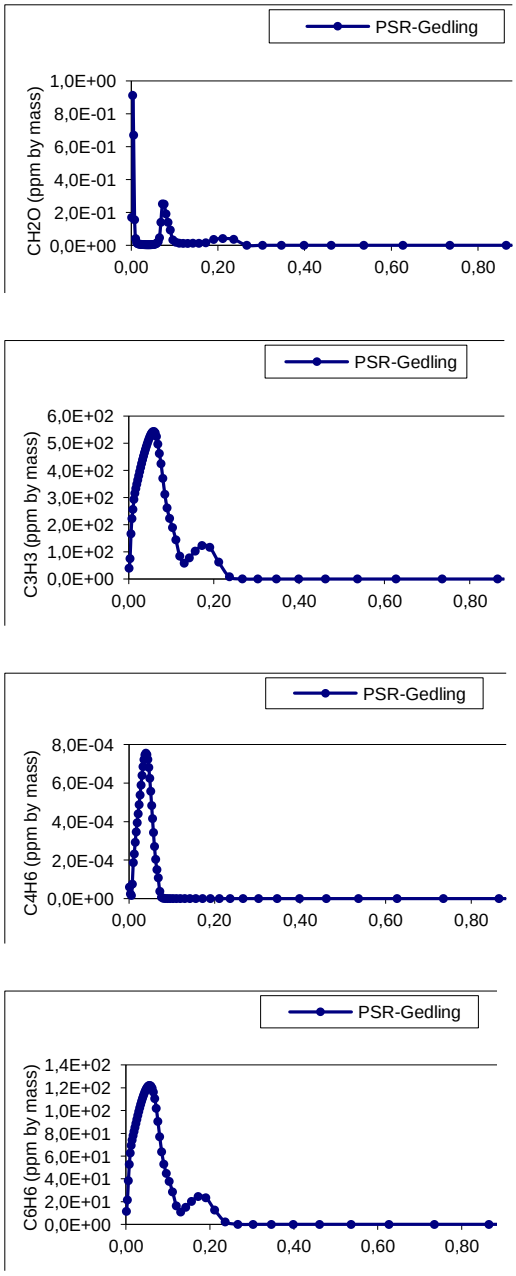

Fig. 13. PSR-Gedling, Axial Profile of Important VOCs Species.

Figures 13-14 illustrate the concentration of some of the VOCs. All these figures demonstrate a narrow formation and destruction window. The maximum peak level is around 120 ppm for benzene and 0.6 ppm for formaldehyde, around 450 ppm for propagyle and insignificant level for 1,3-butadiene. The fast destruction takes place in the narrow corridor between the reverse flow and the incoming secondary air stream. The concentration of VOCs in the NBR is the result of devolatilisation and consumption due to gas phase combustion. There is a very narrow window in which we can observe high concentrations of VOCs in the internal recirculation zone near the quarl exit where most of the volatiles are released from the coal particles. The second peak in concentration due to devolatilisation of the large particle size

groups is observed 0.165 m downstream of the burner exit or approximately 4 burner diameters. Therefore, there are narrow peaks of propagyl and benzene concentrations in these regions. The region of high concentration appears to be small and intense due to transportation by the strong reverse flow. The sharp gradient in the concentration of VOCs is due to the effect of the shear mixing zone between the internal reverse flow and the incoming secondary flow. Thereby this leads to a high rate of VOCs consumption, as evident from the concentration curves. The intense combustion of volatiles inside the quarl consumes a substantial amount of hydrocarbons up to 0.2 m from the burner. Therefore, most of volatile organic compounds are consumed in this region as well.

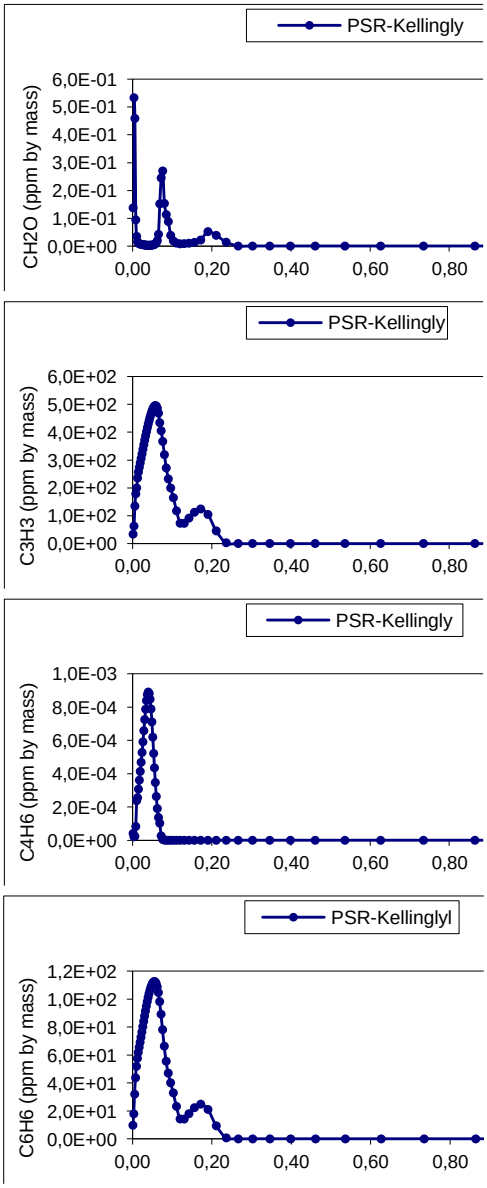

Fig. 14. PSR-Kellingly, Axial Profile of Important VOCs Species.

Simulations show that self-combination of propargyl radicals is the main route leading to benzene in the early flame region. Furthermore, it can be seen from the 1,3-butadiene graphs that the amount of 1,3-butadiene is not sufficient to make a significant contribution to the overall benzene concentration. When the benzene graphs are compared, it is clearly seen that where there is an abundance of propagyle, there a high concentration of benzene appears as well. This observation is confirmed by some other investigators (Miller and Melius, 1992; Lueng, 1995, and D'Anna *et al*., 2000). These researchers observed that the main channel of formation of benzene from small species is propagyle and the contribution of 1,3-butadiene is insignificant. This can be seen the graphs of 1,3-butadiene, as the concentration of 1,3-butadiene is insignificant compared with propagyle concentrations. It can be seen from axial profiles of benzene prediction of Kellingly coal that there is discrepancy between predictions and experimental results (Fig. 15). The reaction mechanism is based on light hydrocarbon fuels, namely methane and acetylene fuel mixing. Therefore, it is expected to underpredict the benzene concentration since some benzene may be produced at the beginning of devolatilasition process because of the nature of the coal's aromatic contents.

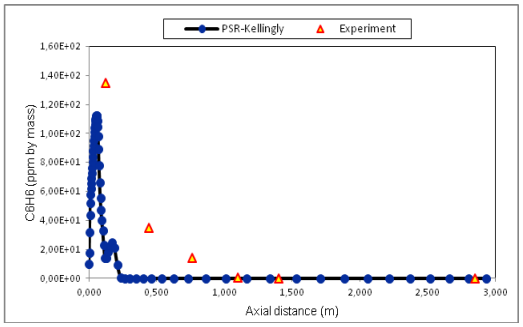

Fig. 15. Validation of Benzene Predictions for Kellingly, Axial Profile.

A concentration of formaldehyde can be explained as the result of two processes. In the first some of C_1 species can result in a breaking-up into smaller species because of oxidation and the pyrolysis processes. The second is possibly a result of the recombination of small molecular species that are transported from the NBR region to downstream by convection. Diffusion processes may have a small contribution as well. However, like benzene, formaldehyde is produced and rapidly consumed in a very narrow window.

6. CONCLUSIONS

The quality of the combustion predictions is reasonably accurate, for both of Gelding and Kellingly coals, especially in the near burner zone, where most of the combustion takes place. A comparison of the performances of the PSR-VOC model against the large laboratory scale experimental data has resulted in considerable confidence in the use of this model for a full-scale boiler configuration. Obviously, more confidence will be forthcoming from an increase in the amount of validation data, which is unluckily lacking at the

moment. In conclusion, the PSR-VOC model has an attractive feature in that it is computationally less expensive. However, small perturbations of these minute concentration levels in the system (ppm level) can affect the accuracy of the prediction. The model can be used in a way that can provide deeper insight into the formation processes of VOC species. This can be accomplished by including more elementary reactions into the reaction mechanisms and by applying the PSR-VOC model.

REFERENCES

Abbas, A. S. and F. C. Lockwood (1988). Prediction of power station combustors. *Twenty-First Symposium (International) on Combustion* 21(1), 285-92.

Abbas, T. (1993). *In Flame Measurements of N-Pollutants and Burnout in a Pulverized Coal Fired Furnace*. Ph.D. thesis, Imperial College, the University of London. London.

Alkemade, U. and K. H. Homann (1989). Formation of C6H6 Isomers by Recombination of Propynyl in the System Sodium Vapor Propynylhalide. *Zeitschrift fur Physikalische Chemie Neue Folge Part* 161(1-2), 19-34.

Anthony, D. B. And J. B. Howard, J.B. (1976). Coal Devolatilisation and Hydrogasification. *AIChE Journal* 22(4), 625-656.

Arslan, Ö. (2015). The Impact of the Release of VOCs and PAHs from Power Stations on the Environment and Human. *13th International Combustion Symposium*, 9-11 September, Bursa-Turkey.

Baulch, D. L., C. J. Cobos, R. A. Cox, C. Esser, P. Frank, Th. Just, J. A. Kerr, M. J. Pilling, J. Troe, R. W. Walker and J. Warnatz (1992). Evaluated Kinetic Data for Combustion Modelling. *Journal of Physical and Chemical Reference Data* 21(3), 411-734.

Baulch, D. L., C. J. Cobos, R. A. Cox, P. Frank, G. Hayman, T. Just, J. A. Kerr, T. Murrells, M. J. Pilling, J. Troe, R. W. Walker and J. Warnatz **(**1994). Summary Table of Evaluated Kinetic Data for Combustion Modeling: Supplement I. *Combustion and Flame* 98(1-2), 59-79.

Benson, S. W. (1989). The Mechanism of the Reversible Reaction: 2C2H2 = Vinyl Acetylene and the Pyrolysis of Butadiene. *International Journal of Chemical Kinetics* 21, 233-243.

Bittker, D. A. (1991). Detailed Mechanism for Oxidation of Benzene. *Combustion Science and Technology* 79(1-3), 49-72.

Böhland, T. and F. Temps (1984). Direct Determination of the Rate-Constant for the Reaction CH2 + H = CH + H2. *Berichte Der Bunsen-Gesellschaft-Physical Chemistry Chemical Physics* 88, 459-461.

Borghi, R. (1988). Turbulent Combustion Modelling. *Progress in Energy and Combustion Science* 14(4), 245-292.

Brown, P. N., G. D. Byrne and A. C. Hindmarsh, (1989). VODE: A Variable Coefficient ODE Solver. *SIAM Journal on Scientific and Statistical Comput*ing 10(5), 1038-1051.

Burden, R. L., J. D. Faires and A. M. Burden (2015). *Numerical Analysis*, 10th ed. Boston: Cengage Learning.

Byrne, G. D. and A. C. Hindmarsh (1976). *EPISODEB: An Experimental Package for the Integration of Systems of Ordinary Differential Equations with Banded Jacobians*. LLNL Report UCID-30132.

Byrne, G.D. and A. C. Hindmarsh (1975). A Polyalgorithm for the Numerical Solution of Ordinary Differential Equations. *ACM Transaction on Mathematical Software(TOMS)* 1(1), 71-96.

Chagger, H. K., J. M. Jones, M. Pourkashanian, A. Williams, A. Owen and G. Fynes (1999). Emission of Volatile Organic Compounds from Coal Combustion. *Fuel* 78(13), 1527-38.

Costa, M, P. Costen, F. C. Lockwoodand T. Mahmud (1990). Detailed Measurements in and Modelling of an Industry-Type Pulverised Coal Flame. *22nd Symposium (International) on Combustion* 22(1), 973-980.

Costa, M. M. G. (1992). *On Combustion of Heavy Fuel Oil and Pulverised Coal in a Large Scale Laboratory Furnace*. Ph. D. thesis, Imperial College, the University of London. London.

D'Anna, A., A. Violi and A. D'Alessio (2000). Modeling the Rich Combustion of Aliphatic Hydrocarbons. *Combustion and Flame* 121(3), 418–429.

Diprima, W. E. And R. C. Boyce (2012). *Elementary Differential Equations and Boundary Value Problems*. 10th ed. John Wiley and Sons, New York:

Emdee, J. L., K. Brezinsky and I. A. Glassman (1992). Kinetic Model for the Oxidation of Toluene near 1200 K. *Journal of Physical Chemistry* 96(5), 2151-2216.

Fernandez-Martinez, G., J. M. Lopez-Vilarino, P. Lopez-Mahia, S. Muniategui-Lorenzo, D. Prada-Rodríguez and E. Fernandez-Fernandez (2001). Determination of volatile organic compounds in emissions by coal-fired power stations from Spain. *Environmental Technology* 22(5), 567-75.

Ferziger, J. H. and M. Peric (2013). *Computational Methods for Fluid Dynamics*, 3rd Edition, Springer.

Fox, R. O. and J. Villermaux (1990). Unsteady-State IEM Model: Numerical Simulation and Multiple-Scale Perturbation Analysis near Perfect-Micromixing Limit. *Chemical*

Engineering Science 45(2), 373-86.

Garcia, J. P., S. Beyne-Masclet, G. Mouvier and P. Masclet (1992). Emissions of Volatile Organic Compounds by Coal-Fired Power Stations. *Atmospheric Environment* 26A:1589-97.

Gibb, J. (1973). *Central Electricity Board*, Internal note, MRM 85.

Grotheer, H. H., S. Kelm, H. S. T. Driver, R. J. Hutcheon, R. D. Locket and G. N. Robertson (1992). Elementary Reactions in the Methanol Oxidation System. Part 1:Establishment of the Mechanism and Modelling of Laminar Burning Velocities. *Berichte Der Bunsen-Gesellschaft-Physical Chemistry Chemical Physics* 96(10), 1360-1376

Harrison, P. J. (2002). *In Flame Measurement of Specific VOCs from Combustion of Pulverised Fossil and Renewable Fuels*. Ph. D. thesis, Imperial College, the University of London. London.

Hassan, S. (1997). *Emissions of Nitrogen Oxides, Particulates and Toxic Metals from Fossil and Waste Fired combustors*. Ph. D. thesis, Imperial College, the University of London, London.

Hindmarsh, A. C. (1983). *ODEPACK, a Systematized Collection of ODE Solvers*. In: Stepleman R. S. et al., editors. In Scientific Computing, Amsterdam: North-Holland Publishing Co; 55-64.

Hindmarsh, A. C. and G. D. Byrne (1977). *EPISODE: An Effective Package for the Integration of Systems of Ordinary Differential Equations*. LLNL Report UCID-30112, Rev. 1.

Homann, K. H., and Ch. Wellmann (1983). Arrhenius Parameters for the Reactions of O Atoms with Some Alkynes in the Range 300-1300 K. *Berichte der Bunsengesellschaft/Physical Chemistry Chemical Physics* 87(6), 527-532.

Kang, Y. S., S. S. Kim and S. C. Hong (2015). Combined process for removal of SO_2, NO_x, and particulates to be applied to a 1.6-MWe pulverized coal boiler. *Journal of Industrial and Engineering Chemistry* 30, 197-203.

Kern, R. D., C. H. Wu, G. B. Skinner, V. S. Rao, J. H. Kiefer, J. A. Towers and L. J. Mizerka (1985). Collaborative shock tube studies of benzene pyrolysis. *Twentieth Symposium (International) on Combustion* 20(1), 789-797.

Kiefer, J. H., L. J. Mizerka, M. R. Patel and H. C. Wie (1985). A Shock Tube Investigation of Major Pathways in the High-Temperature Pyrolysis of Benzene. *Journal of Physical Chemistry* 89(10), 2013-2019.

Kiefer, J. H., S. S. Sidhu, R. D. Kern, K. Xie, H. Chen and L. B. Harding (1992). The Homogeneous Pyrolysis of Acetylene.2, the High-Temperature Radical Chain Mechanism. *Combustion Science and Technology* 82(1-6), 101-130.

Lam, F. W., J. P. Longwell and J. B. Howard (1991). The Effect of Ethylene and Benzene Addition on the Formation of Polycyclic Aromatic Hydrocarbons and Soot in a Jet-Stirred/Plug Flow Combustor. *23rd Symposium (International) on Combustion* 23(1), 1477-1484.

Launder, B. E. and D. B. Spalding, (1974). Numerical Calculation of Turbulent Flows. *Computer Methods in Applied Mechanics and Engineering* 3, 269-289.

Leidreiter, H. I. and H. G. Wagner, (1989). An Investigation of the Reaction between O and Benzene at High Temperatures. *Z. Phys. Chem. Neue Folge* 165(1), 1-7.

Levy, J. F. (1991). *Prediction of Flow, Combustion and Heat Transfer in Coal Fired Cement Kilns*. Ph. D. thesis, Imperial College, the University of London. London.

Lin, C. Y. and M. C. Lin (1986). Thermal Decomposition of Methyl Phenyl Ether in Shock Waves: The Kinetics of Phenoxy Radical Reactions. *Journal of Physical Chemistry* 90(3), 425-431.

Lindstedt, R. P. and G. Skevis (1997). Chemistry of Acetylene Flames. *Combustion Science and Technology* 125(1-6), 73-137.

Lindstedt, R. P. and G. Skevis, G. (1994). Detailed Kinetic Modelling of Premixed Benzene Flames. *Combustion and Flame* 99(3-4), 551-561.

Liu, A., W. A. Mulac and C. D. Jonah (1988). Rate constants for the gas-phase reactions of OH radicals with 1,3-butadiene and allene at 1 atm in Ar and over the temperature range 305-1173 K. *Journal of Physical Chemistry* 92(1), 131-134.

Lockwood, F. C. and A. P. Salooja (1983). The prediction of some pulverized bituminous coal flames in a furnace. *Combustion and Flame* 54(1-3), 23-32.

Lockwood, F. C. and B. Shen (1994). Performance Predictions of Pulverised-Coal Flames of Power Station Furnace and Cement Kiln Type. *25th Symposium (International) on Combustion* 25(1), 503-505.

Lockwood, F. C. and C. A. Romo-Millares (1992). Mathematical Modelling of Fuel-NO Emissions from PF Burners. *Journal of the Institute of Energy* 65(464), 144-152.

Lockwood, F. C. and T. Mahmud (1988). Prediction of the Swirl Burner Pulverised Coal Flames. *22nd Symposium (International) on Combustion* 22(1), 165-173.

Lockwood, F. C., A. P. Solooja and S. A. Syed (1980). A Prediction Method for Coal Fired

Furnaces. *Combustion and Flame* 38(1), 1-15.

Longwell, J. P. and M. A. Weiss (1955). High Temperature Reaction Rates in Hydrocarbon Combustion. *Industrial Engineering Chemistry* 47(8), 1634-1643.

Lueng, K. M. (1995). *Kinetic Modeling of Hydrocarbon Flames Using Detailed and Systematically Reduced Chemistry*. Ph. D. thesis, Imperial College, the University of London. London.

Lueng, K. M. and R. P. Lindstedt (1995). Detailed Kinetic Modeling of C1 and C3 Alkane Diffusion Flames. *Combustion and Flame* 102(1-2), 129-60.

Magnussen, B. F. and B. H. Hjertager (1976). On Mathematical Models of Turbulent Combustion with Special Emphasis on Soot Formation and Combustion. *16th Symposium (International) on Combustion* 16(1), 719-729.

Mantel, T. and R. Borghi **(**1994). A new model of premixed wrinkled flame propagation based on a scalar dissipation equation. *Combustion and Flame* 96(4), 443-457.

Marr, J. A., L. M. Giovane, J. P. Longwell, .J. B. Howard and A. L. Lafleur (1994). Soot and Tar Production in a Jet-Stirred/Plug-Flow Reactor System: High and Low C2H2 Concentration Environments. *Combustion Science and Technology* 101(1-6), 301-09.

Masclet, P., M. A. Bresson and G. Mouvier (1987). PAHs emitted by Power Stations, and Influence of Combustion Conditions. *Fuel* 66(4):556-562.

Michael, J. V. and K. P. Lim (1993). Shock Tube Techniques in Chemical Kinetics. *Annual Review of Physical Chemistry* 44(1), 429-458.

Miller, J. A. and C. F. Melius (1992). Kinetic and Thermodynamic Issues in the Formation of Aromatic-Compounds in Flames of Aliphatic Fuels. *Combustion and Flame* 91(1), 21-39.

Patankar, S. V. (1980). *Numerical Heat Transfer and Fluid Flow*. Hemisphere Publishing Corporation, Washington.

Pisupati, S. V., R. S. Wasco and A. W. Scaroni (2000). An investigation on polycyclic aromatic hydrocarbon emissions from pulverized coal combustion systems. *Journal of Hazardous Materials* 74(1), 91-107.

Revuelta, C. C., E. D. L. F. Santiago and J. A. R. Vazquez (1999). Characterization of polycyclic aromatic hydrocarbons in emissions from coal-fired power plants: The influence of operation parameters. *Environmental Technology* 20(1), 61-8.

Richter, H. and J. B. Howard (2000). Formation of Polycyclic Aromatic Hydrocarbons and their Growth to Soot—a Review of Chemical Reaction Pathways. *Progress in Energy and Combustion Science* 26(4-6), 565-608.

Righter, H., W. J. Grieco and J. B. Howard (1999). Formation, Mechanism of Polycyclic Aromatic Hydrocarbons and Fullerenes in Premixed Benzene Flames. *Combustion and Flame* 119(1-2), 1-22.

Rizvi, S. M. A. (1985). *Prediction of Flow, Combustion and Heat Transfer in Pulverised Coal Flames*. Ph. D. thesis, Imperial College, the University of London. London.

Rogg, B. (1988). Response and Flamelet Structure of Stretched Premixed Methane-Air Flames. *Combustion and Flame* 73(1), 45-65.

Skevis, G. (1996). *Soot Precursor Chemistry in Laminar Premixed Flames*. Ph. D. thesis, Imperial College, the University of London. London.

Slagle, I. R., G. W. Gmurczy, L. Batt and D. Gutman **(**1991). Kinetics of the Reaction between Oxygen Atoms and Propargyl Radicals. *23rd Symposium (International) on Combustion* 23(1), 115-121.

Smooke, M. D. (1991). *Reduced Kinetic Mechanisms and Asymptotic Approximations for Methane Flames*, Lecture Notes in Physics 384. Springer-Verlag.

Takahashi, F., J. W. Blust, J. Zelina, R. C. Striebich and C. W. Frayne (1995). Soot Threshold Measurements Using a Well-Stirred Reactor. *Combustion Institute (Eastern States Section)* 431-434.

Timonen, R. S., E. Ratajczak, D. Gutman and A. F. Wagner (1987). The Addition and Dissociation Reaction H + O_2 = HCO. 2. Experimental Studies and Comparison with Theory. *Journal of Physical Chemistry* 91, 5325-5332.

Tregrossi, A., A. Ciajolo and R. Barbella (1999). The Combustion of Benzene in Rich Premixed Flames at Atmospheric Pressure. *Combustion and Flame* 117(3), 553-561.

Tsang, W. and R. F. Hampson (1986). Chemical Kinetic Data Base for Combustion Chemistry. Part 1. Methane and Related Compounds. *Journal of Physical and Chemical Reference Data* 15(3), 1087-1279.

Vaughn, C. B., J. B. Howard and J. P. Longwell (1991). Benzene Destruction in Fuel-Rich Jet Stirred Reactor Combustion. *Combustion and Flame* 87(3-4), 278-288.

Versteeg, H. K. and W. Malalasekera (2007). *An Introduction to Computational Fluid Dynamics*. 2nd. Ed., Pearson Education Limited.

Villermaux, J. (1986). Micromixing Phenomena in Stirred Reactors. In: Cheremisinoff NP, editor. *Encyclopedia of Fluid Mechanics: Dynamics of Single Fluid Flows and Mixing (Volume 2), chapter 27, Huston*. Gulf Publishing Company p.707-768.

Violi, A., A. D'Anna and A. D'Alessio (1999). Modeling of Particulate Formation in Combustion and Pyrolysis. *Chemical Engineering Science* 54(15-16), 3433-3442.

Wang, H. and M. Frenklach (1994). Calculations of Rate Coefficients for the Chemically Activated Reactions of Acetylene with Vinylic and Aromatic Radicals. *Journal of Physical Chemistry* 98(44), 11465-11489.

Wang, H. and M. Frenklach (1997). A Detailed Kinetic Modelling Study of Aromatics Formation in Laminar Premixed Acetylene and Ethylene Flames. *Combustion and Flame* 110(1-2), 173-221.

Warnatz, J. (1981). The Structure of Laminar Alkane, Alkene, and Acetylene Flames. *18th Symposium (International) on Combustion* 18(1), 369-84.

Warnatz, J. (1984). Rate Coefficients in the C/H/O System. In: Gardiner Jr W. C. editor. *Combustion Chemistry*, New York: Springer-Verlag; p.197-360.

Warnatz, J. (1992). Resolution of Gas Phase and Surface Combustion Chemistry into Elementary Reactions. *24th Symposium (International) on Combustion* 24(1), 553-79.

Wei, X. L., X. F. Guo, S. Li, X. H. Han, U. Schnell, G. Scheffknecht and B. Risio (2012). Detailed Modeling of NOx and SOx Formation in Co-*Combustion* of *Coal* and Biomass with Reduced Kinetics. *Energy & Fuels* 26(6):3117-24.

Weissman, M. A. and S. W. Benson (1988). Rate parameters for the reactions of C_2H_3 and C_4H_5 with H_2 and C_2H_2. *Journal of Physical Chemistry* 92(14), 4080-4084.

Westbrook, C. K. and W. J. Pitz (1984). A Comprehensive Chemical Kinetic Reaction-Mechanism for Oxidation and Pyrolysis of Propane and Propene. *Combustion Science and Technology* 37(3-4), 117-152.

Westmoreland, P. R. (1992). Thermochemistry and Kinetics of C2H3 + O2 Reactions. *Combustion Science and Technology* 82(1-6), 151-168.

Yamazaki, H. and A. Ichikawa (1970). Stability of a Dispersed-Phase Chemical Reactor and the Effect of Coalescence and Redispersion of Dispersed Drops. *International Chemical Engineering* 10:471-478.

Yehia, M. (1992). *Modelling of Pulverised Coal Swirling Flames in Axi-Symmetric Furnaces*. Ph. D. thesis, Imperial College, the University of London. London.